J|A|C|S
COMMUNICATIONS

Published on Web 12/14/2002

Layer-By-Layer Growth of Metal−Metal Bonded Supramolecular Thin Films and Its Use in the Fabrication of Lateral Nanoscale Devices

Chun Lin* and Cherie R. Kagan*

IBM T. J. Watson Research Center, P.O. Box 218, Route 134, Yorktown Heights, New York 10598

Received September 23, 2002; E-mail: cheriek@us.ibm.com; chunlin@tamu.edu

Metal−metal bonded units with the "paddlewheel" framework have been employed to build supramolecular arrays.[1] A series of neutral complexes with both discrete and extended structures have been synthesized from a "subunit-linker" combinatorial library. Most of these compounds undergo multiple redox processes without loss of structural integrity and display extensive electronic coupling between M_2 centers. Previous studies have suggested that the half-wave potentials of these redox reactions can be both significantly and precisely tuned by the substitutents at the ligand periphery.[2] However, to date efforts to investigate these metal−metal bonded complexes have been limited to solution-based systems. To harness the electronic, optical, and magnetic properties of these materials in solid-state applications and devices, development of new methods for making thin films containing functional metal−metal bonded complexes are needed.

In particular, the rich electrochemistry makes these materials interesting in molecular junctions. Two-terminal vertical molecular devices[3] require metal to be deposited on top of the molecular layer, often leading to shorted junctions through defects and to unknown and uncharacterized interfaces between the metal electrode and the molecules. Lateral device structures that do not require the top metal deposition have recently been reported.[4] Presently e-beam lithography provides the simplest route to fabricate electrodes with small spacings, but the smallest reported separations are ∼6−10 nm,[5] much larger than many molecules that are short enough to be soluble and that may be of interest. Layer-by-layer growth has been demonstrated as a route to assemble multilayer metal−ligand structures.[6] In this communication, we report the layer-by-layer growth of a new system of inorganic coordination complexes, namely metal−metal bonded supramolecules, and the fabrication of nanoscale lateral devices by templating the growth of such supramolecules from electrodes separated by 60−80 nm until they meet in the middle of the gap.

Layer-by-layer growth of metal−metal bonded compounds is exemplified by the infinite tubular molecule, $\{[Rh_2(DAniF)_2]_2(O_2CCH_2CO_2)_2(NC_5H_4CHCHC_5H_4N)_2\}_n$ (DAniF = *N*,*N*′-di-*p*-anisylformamidinate), made by employing molecular loop **1** (Scheme 1) and the axial linker *trans*-1,2-bis(4-pyridyl)ethylene, **2**. This molecule has previously been synthesized and structurally characterized in single-crystal form.[7] A monolayer of 4-pyridylethylmercaptan was first self-assembled on the substrate from an ethanol solution.[8] The assembly of molecular loop **1** was then templated on this pyridyl-terminated surface by dipping in 0.1 mM toluene solution at −15 °C for 1 h through the strong interaction between Rh and N atoms. Following the initial deposition of **1**, the second layer consisting of a dipyridyl ethylene linker coordinates the axial positions of Rh−Rh bonds by soaking in a 0.1 mM ether solution of **2** for 10 min. Alternate dipping into these two solutions is used to build multilayer assemblies. After the first bilayer is formed, dipping times for both solutions can be reduced to 1 min, since the longer dipping times do not show any change in UV−vis spectra.

Scheme 1

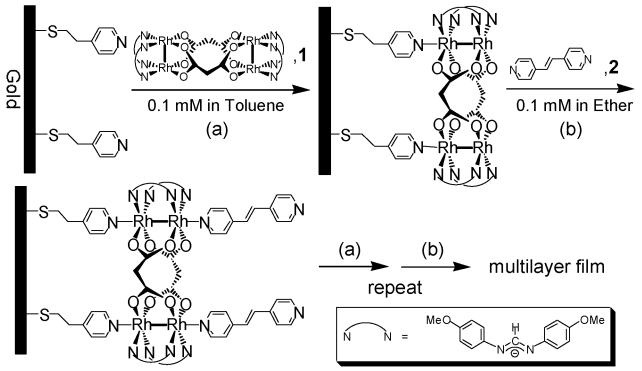

The excess compounds on the surface are removed by copious washing between each dipping in toluene for **1** and ether for **2**. The formation of **1** at low temperature is essential to prevent dissolution of the linker **2** back into solution.

Film growth was monitored by UV−vis spectroscopy, as shown in Figure 1. The peaks at 258 and 298 nm correspond to the characteristic absorptions of **1** and **2**, respectively. The linear increase in absorbance as a function of the number of added bilayers indicates that the same amount of material is being deposited in each dipping cycle. Assuming that the solution ϵ_{max} values are the same as those of the two-dimensional surface extinction coefficients, the calculated average bilayer coverage of the film is $\sim 0.9 \times 10^{-10}$ mol/cm^2 and the ratio of **1** to **2** is 1:2. This value is consistent with that of 1.0×10^{-10} mol/cm^2 obtained from the single-crystal X-ray structure,[7] suggesting that the film formation is packed as in the bulk solid.

The thickness of the films was evaluated by atomic force microscopy (AFM) using a step edge in the substrate to provide an internal standard. The step edge was fabricated by selectively etching into a photolithographically patterned SiO_2 (400 Å) on Si wafer, using the wafer as an etch stop, evaporating Au/Ti, and lifting-off the resist. Figure S1 shows the increase in assembly thickness as a function of the number of bilayers, together with the corresponding AFM images near the step edge. The best-fit line gives a slope of 1.5 nm, corresponding to the average bilayer thickness, and an intercept of 1.4 nm, corresponding to the thickness of the thiolate monolayer. X-ray structure analysis on single crystals of the analogous compound yields a length of 1.61 nm for each bilayer. Our results suggest that the molecular tube formed in the film is nearly perpendicular to the substrate surface. Film roughnesses of 0.62 and 0.56 nm were found for 5 and 20 bilayers, respectively (Figure S2), less than a monolayer thickness.

In all dirhodium formamidinate compounds the Rh_2^{4+} unit can undergo two one-electron reversible oxidation processes.[9] Thin films grown on Au surfaces have been examined by cyclic voltammetry in 1 M NaCl aqueous solutions. The results for 5 bilayers are displayed in Figure 2. The oxidation potential of Rh_2^{4+} to Rh_2^{5+} in

10.1021/ja028653y CCC: $25.00

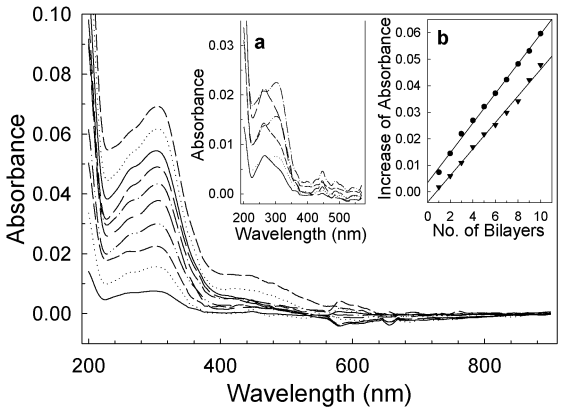

Figure 1. UV−vis spectra of bilayer films as multilayers are assembled increasing the film thickness from 1 to 10 bilayers. (Inset) (a) UV−vis spectra of the first three bilayers (total six monolayers) showing the alternative addition of **1** (at 258 nm) and **2** (at 298 nm). (b) Increase in absorbance at 258 (circles) and 298 (triangles) nm as a function of the number of added bilayers

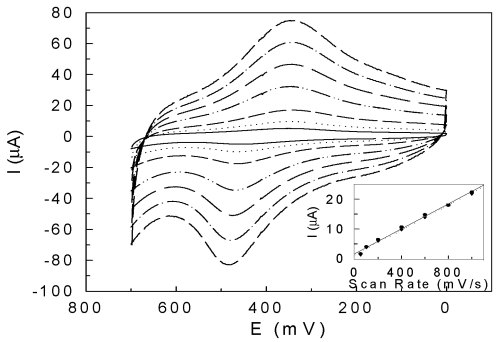

Figure 2. Cyclic voltammograms of a five-bilayer film on a Au substrate with scan rates of (from inside to outside) 50, 100, 200, 400, 600, 800, and 1000 mV/s. (Insert) Plot of i_{pa} and i_{pc} vs scan rate.

bilayer films occurs at 406 mV vs Ag/AgCl, according to $E_{1/2} = (E_{pa} + E_{pc})/2$, close to that found for compound **1** in CH_2Cl_2 solutions (365 mV). The E_{pa} and E_{pc} values remain unchanged with a separation of 116 mV, and the peak currents show a linear dependence with scan rate between 50 and 1000 mV/s. Peak shapes are invariant with repetitive cycling. These results indicate that the molecular tubes in the bilayer films are a surface-bound, unusual quasi-reversible redox active species.[10] The second oxidation of the Rh_2 core is not visible due to the solvent limit under current experimental conditions. The above film growth method has also been demonstrated on oxide substrates and with different axial linkers, such as zinc 5,10,15,20-tetra(4-pyridyl)-21*H*,23*H*-porphine.[11]

Utilizing the above layer-by-layer directed assembly method, we have fabricated lateral devices. In a typical experiment, electrodes (18 nm Au-on-2 nm Ti) with 60−80 nm gaps were prepared by e-beam lithography on oxidized Si wafers. Following the same deposition procedures described above, assemblies consisting of **1** and **2** are grown off the metal electrodes, narrowing the measured gap and spanning the spacing between electrodes as the number of bilayers are increased. This process is monitored by AFM as shown in the images (Figures 3b) and in the corresponding cross-sections (Figure 3c). Once the electrode gap is spanned by the metal−metal bonded compounds representative $I-V$ characteristics akin to

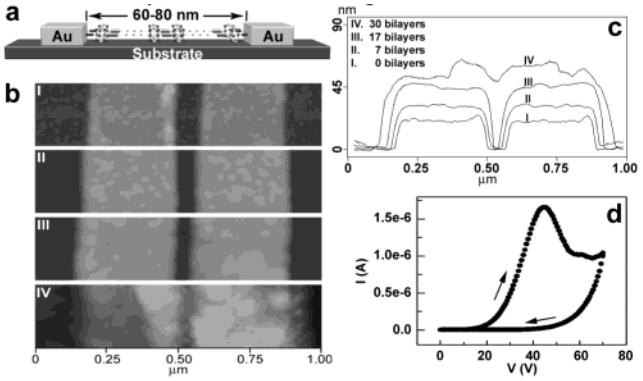

Figure 3. Fabrication of the device. (a) Device structure, (b) AFM images showing the closing of the gap while increasing the number of bilayers, (c) cross-sections of their corresponding AFM images, (d) $I-V$ curve.

voltage-controlled negative differential resistance, as shown in Figure 3d, are attained. This $I-V$ curve is only observed in the first cycling of the device, but is reproducible from device-to-device on the same chip and devices on different chips. We speculate that the characteristics arise from oxidation of the Rh_2 units, consistent with the voltage drop across each dimetal unit as observed electrochemically, but that it is irreversible in the solid state or in this symmetric device configuration.

In summary, we have demonstrated the layer-by-layer assembly of metal−metal bonded molecules to form thin films that may be directed on different substrate surfaces using monolayer templates. These thin film structures and their physical properties, such as half-wave redox potentials, may be tuned by choosing from a broad range of metals and equatorial and axial linkers. The application of these multilayers as active materials for switching and other molecular devices is currently being investigated.

Supporting Information Available: Figure S1 (AFM measurements of thin film thickness), Figure S2 (AFM images of thin films with 5 and 20 bilayers) (PDF). This material is available free of charge via the Internet at http://pubs.acs.org.

References

(1) (a) Cotton, F. A.; Lin, C.; Murillo, C. A. *Acc. Chem. Res.* **2001**, *34*, 759. (b) Cotton, F. A.; Lin, C.; Murillo, C. A. *Proc. Natl. Acad. Sci. U.S.A.* **2002**, *99*, 4810.
(2) Ren, T. *Coord. Chem. Rev.* **1998**, *175*, 43.
(3) (a) Chen, J.; Reed, M. A.; Rawlett, A. M.; Tour, J. M. *Science* **1999**, *286*, 1550. (b) Collier, C. P.; Mattersteig, G.; Wong, E. W.; Luo Y.; Beverly, K.; Sampaio, J.; Raymo, F. M.; Stoddart, J. F.; Heath, J. R. *Science* **2000**, *289*, 1172.
(4) (a) Park, J.; Pasupathy, A. N.; Goldsmith, J. I.; Chang, C.; Yalsh, Y.; Petta, J. R.; Rinkoski, M.; Sethna, J. P.; Abruna, H. D.; McEuen, P. L.; Ralph, D. C. *Nature* **2002**, *417*, 722. (b) Liang, W.; Shores, M. P.; Bockrath, M.; Long, J. R.; Park, H. *Nature* **2002**, *417*, 725.
(5) Guillorn, M. A.; Carr, D. W.; Tiberio, R. C.; Greenbaum, E.; Simpson, M. L. *J. Vac. Sci. Technol., B* **2000**, *18*, 1177.
(6) (a) Cao, G.; Hong, H. G.; Mallouk, T. E. *Acc. Chem. Res.* **1992**, *25*, 420. (b) Decher, G. *Science* **1997**, *277*, 1232. (c) Putvinski, T. M.; Schilling, M. L.; Katz, H. E.; Chidsey, C. E. D.; Mujsce, A. M.; Emerson, A. B. *Langmuir* **1990**, *6*, 1567. (d) Ansell, M. A.; Cogan, E. B.; Page, C. J. *Langmuir* **2000**, *16*, 1172.
(7) Cotton, F. A.; Lin, C.; Murillo, C. A. *Chem. Common.* **2001**, 11.
(8) We found that a 2-h dipping time for 4-pyridylethylmercaptan produced the maximum coverage of the next layer of metal complexes. Longer dipping times decreased the coverage of **1**, which is probably due to steric hindrance resulting from the denser coverage of the mercaptan layer.
(9) Cotton, F. A.; Walton, R. A. *Multiple Bonds Between Metal Atoms*, 2nd ed.; Clarendon Press: Oxford, 1993.
(10) Feldberg, S. W.; Rubinstein, I. *J. Electroanal. Chem.* **1988**, *240*, 1.
(11) Lin, C.; Kagan, C. R. In preparation.

JA028653Y